2013 NDIA GROUND VEHICLE SYSTEMS ENGINEERING AND TECHNOLOGY SYMPOSIUM
MODELING & SIMULATION, TESTING AND VALIDATION (MSTV) MINI-SYMPOSIUM
AUGUST 21-22, 2013 - TROY, MICHIGAN

STRUCTURAL HEALTH MONITORING OF COMPOSITE ARMOR PANELS USING EMBEDDED ULTRASONIC GUIDED WAVE SENSOR ARRAYS

Cody J. Borigo
Jason Bostron
Joseph L. Rose
Steven E. Owens
FBS, Inc.
State College, PA

Thomas P. Reynolds
Thomas J. Meitzler
TARDEC Electrified Armor Lab
Warren, MI

ABSTRACT

FBS Inc. is working with the TARDEC Electrified Armor Lab to develop a non-destructive structural health monitoring technology for composite armor panels that utilizes an array of embedded ultrasonic sensors for guided wave tomographic imaging. This technology would allow for periodic or real-time monitoring of armor integrity while being minimally intrusive and adding negligible weight. The technology is currently being developed and tested in pseudo composite armor panels and efforts are focused on reducing sensor array density, improving sensor integration procedures, and maximizing system sensitivity to damage. In addition to experimental testing and development, FBS is developing a highly-automated finite element model generation and analysis program to be used in conjunction with Abaqus/Explicit commercial finite element software. This program is specifically dedicated to modeling guided wave propagation in pseudo composite armor panels between embedded ultrasonic sensors. This software will allow TARDEC personnel to further investigate a wide array of sensor configurations and sensor densities and to evaluate the sensitivity of various feature extraction and tomography algorithms to damage of varying form and severity.

INTRODUCTION

Structural health monitoring refers to the periodic monitoring of the state of a structure in order to detect, locate, characterize, and monitor damage or other undesirable changes in the structure [1]. FBS, Inc. is working with the TARDEC Electrified Armor Lab to develop a non-destructive structural health monitoring technology for composite armor panels. The technology utilizes an array of embedded piezoelectric sensors to generate and receive ultrasonic guided waves; the collected signals are processed and used to generate a computed tomography image, which can indicate the presence, location, and severity of damage or other structural changes. This technology would allow for periodic monitoring of armor integrity and measurements could be performed weekly, daily, hourly, or nearly continuously to provide structural health monitoring of composite armor structures in real-time. Embedding ultrasonic sensors within the composite armor panel is advantageous because the form factor of the armor is not affected and the sensors themselves are protected within the structure. The technology is currently being developed and tested in pseudo composite armor panels and efforts are focused on reducing sensor array density, improving sensor integration procedures, and maximizing system sensitivity to damage. In addition to experimental testing and development, FBS is developing a highly-automated finite element model generation and analysis program to be used in conjunction with Abaqus/Explicit commercial finite element software. The program that is being developed is specifically dedicated to modeling guided wave propagation in pseudo composite armor panels with embedded ultrasonic sensors. This software will allow TARDEC personnel to computationally investigate a wide array of sensor configurations, sensor densities, and sensor designs and to evaluate the sensitivity of various feature extraction and tomography algorithms to various forms of damage or varying severity.

UNCLASSIFIED: Distribution Statement A. Approved for public release.

GUIDED WAVE COMPUTED TOMOGRAPHY

Ultrasonic guided waves differ from more-commonly-utilized ultrasonic bulk waves in that they interact with structural boundaries as they propagate; if the proper conditions are satisfied, this interaction creates a transverse resonance condition that allows guided waves to propagate long distances in a structure with full volumetric coverage through the structure's thickness [2], as is shown in Figure 1. These characteristics of guided waves make them excellent candidates for inspecting large areas of a structure with a limited number of discrete sensor locations. Guided wave inspection techniques are rapidly gaining popularity, particularly in the field of pipeline inspection, thanks to their ability to propagate long distances (often as much as 100-300' in one direction) with excellent defect sensitivity [3].

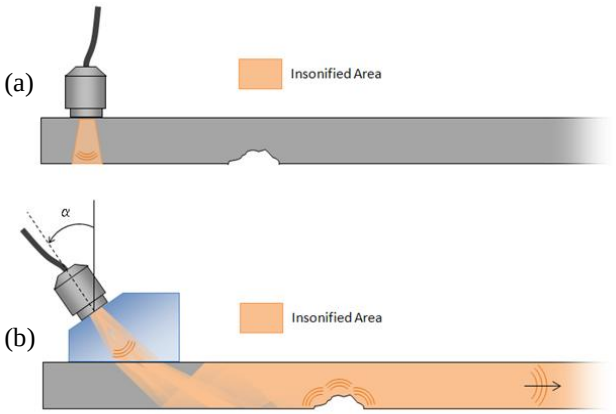

Figure 1: Conceptual illustrations of ultrasonic insonification associated with (a) traditional bulk wave ultrasound and with (b) guided wave ultrasound, in this case excited with an angle beam transducer.

Guided wave computed tomography is a structural health monitoring imaging technique that utilizes an array of distributed pulser-receiver guided wave sensors to generate a two-dimensional pseudo image of damage in a structure, similar to the one shown in Figure 2. To generate this pseudo image, ultrasonic waves are transmitted between each pair of sensors in the array; these signals are compared to a previous data set and analyzed using any number of selected signal processing and feature extraction algorithms to generate a feature value for each sensor pair. Using these feature values, a series of probability of damage distributions, such as the one shown in Figure 3, can be summed and mapped onto a two-dimensional plot representative of the structural area within the bounds of the sensor array [4,5].

The technique's sensitivity to damage, sensitivity to environmental variation (such as temperature fluctuation), and ability to identify the relative severity of damage are dependent on the feature extraction algorithm and other signal processing techniques that are utilized, as well as the sensor design, array design, and pulser-receiver settings utilized during data collection.

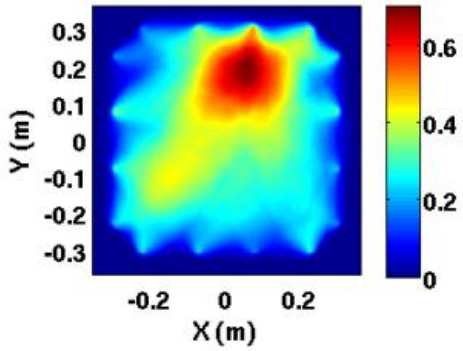

Figure 2: Tomographic image of a 1/8" hole in a 1/2"-thick aluminum plate; the sensor array was 24" by 24" square and contained 16 sensors.

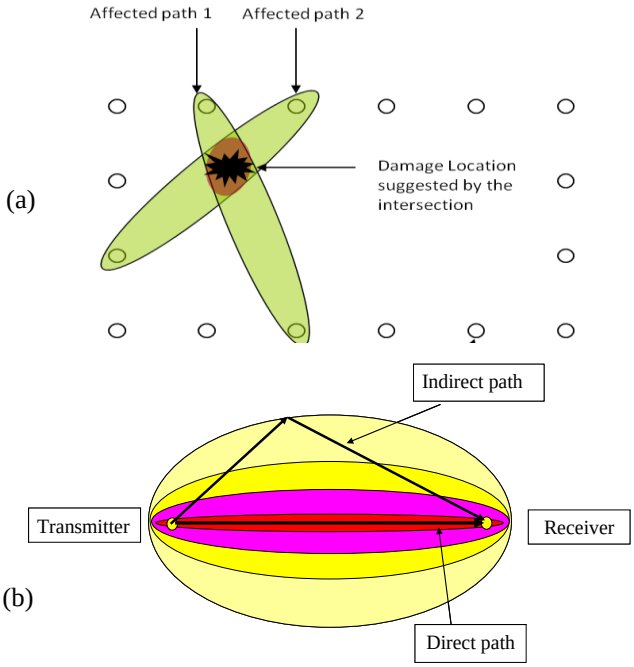

Figure 3: (a) a conceptual illustration of the tomographic imaging technique, and (b) an illustration of the probabilistic damage within a ray effect area described by possible indirect paths between a pair of sensors.

The guided wave tomographic imaging technique can be employed in a number of different embodiments depending on the application and the structural health monitoring data desired by the operator. For composite armor applications, a

guided wave computed tomography system could be utilized as part of a condition-based maintenance program in which a data collection system is periodically plugged into permanently embedded sensors by maintenance personnel to gather guided wave signals and generate tomograms for analysis. Alternatively, the data collection system could be installed in the vehicle and used to monitor the health of the armor panels in near real time during operation.

EXPERIMENTAL RESULTS IN A REPRESENTATIVE ALUMINUM PLATE

To evaluate the relative sensitivity of several signal features to both temperature fluctuation and simulated damage, a series of tomography tests were conducted on a 1/2”-thick aluminum plate, shown in Figure 4. Note that two sensors are located at each position on the aluminum plate in Figure 4. This was for testing purposes only and is not necessary for tomographic imaging. Ultrasonic guided wave signals were collected within a range of temperatures and with a simulated defect having 8 increasing stages of severity, as detailed in Figure 5. The geometry and growth sequence of the defects was selected to act as a loose analogy to damage that may develop in a composite armor panel.

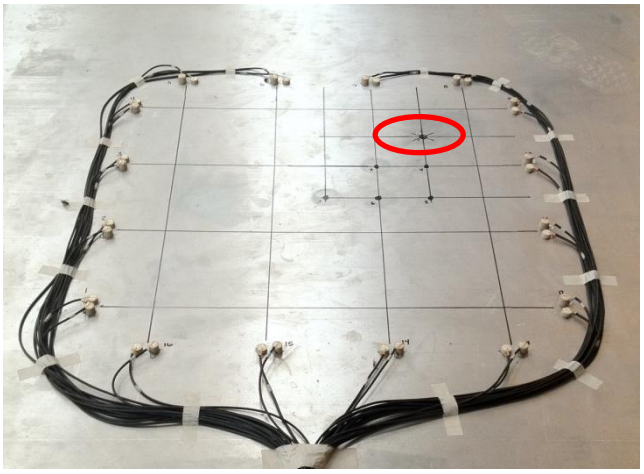

Figure 4: 1/2”-thick aluminum plate with a 24”-by-24” 16-sensor tomography array; the simulated defect is circled in red.

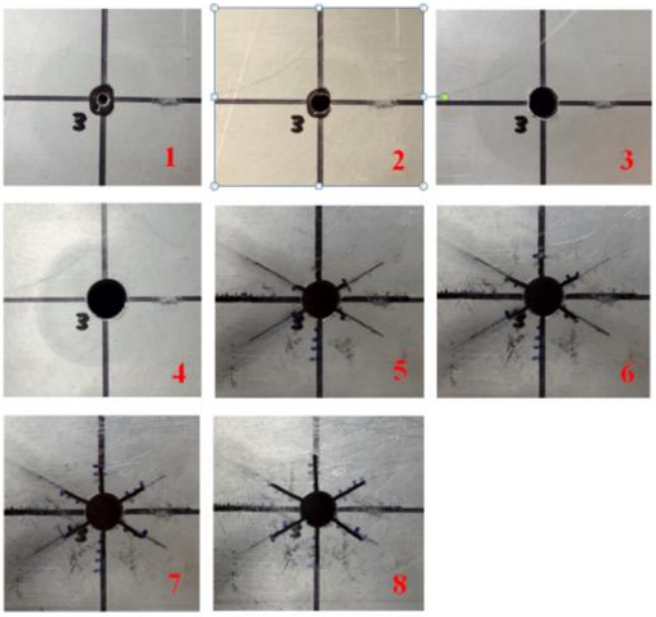

Figure 5: Defect growth stages (from top left to top right, then bottom left to bottom right) – 1/8” hole, 1/4” hole, 3/8” hole, 1/2” hole, 1/2” hole with 1/8” cuts, 1/2” hole with 1/4” cuts, 1/2” hole with 3/8” cuts, 1/2” hole with 1/2” cuts

Signal Feature Comparison – Sensitivity to Damage

The RAPID (reconstruction algorithm for probabilistic inspection of damage) tomography algorithm was utilized for tomogram construction. This algorithm constructs a pseudo-image of damage in the structure by multiplying elliptical defect probability distributions between each pair of sensors, as illustrated in Figure 3b, by a signal change value assigned to each sensor pair. This signal change value, or feature value, can be calculated by a variety of methods. A common method is the signal difference coefficient (SDC) [4], which directly compares two time-domain waveforms using a convolution approach. This feature is typically very sensitive to any defects that may occur in a structure. However, it is also extremely sensitive to changes in boundary conditions and any environmental variations, particularly temperature, due to its heavy reliance on phase information (which is dramatically affected by slight shifts in wave velocities that are often brought about by small temperature changes). In order to determine potential algorithms for use in composite armor panels, several signal features were investigated for tomogram construction using the ultrasonic data collected on the aluminum plate. These features were:

- SDC – the traditional signal difference coefficient
- Hilbert SDC – the SDC of the signal envelope

• FFT SDC – the SDC of the frequency spectrum magnitude
• Envelope peak time – time at which the signal envelope is maximum
• Envelope peak value – maximum amplitude of the signal envelope
• FFT peak frequency – frequency at which the frequency spectrum is maximum
• FFT peak value – maximum amplitude of the frequency spectrum
• Energy – sum of the squares of the discrete time signal

These signal features are in no way all-inclusive, but they represent a broad range of features in the time and frequency domains. Each of these features was used on the same data sets collected from the aluminum panel. Several of the resulting tomograms for the final damage state are shown in Figure 6, including examples of both "good" and "poor" results. Clearly certain signal features detected the damage more accurately than others.

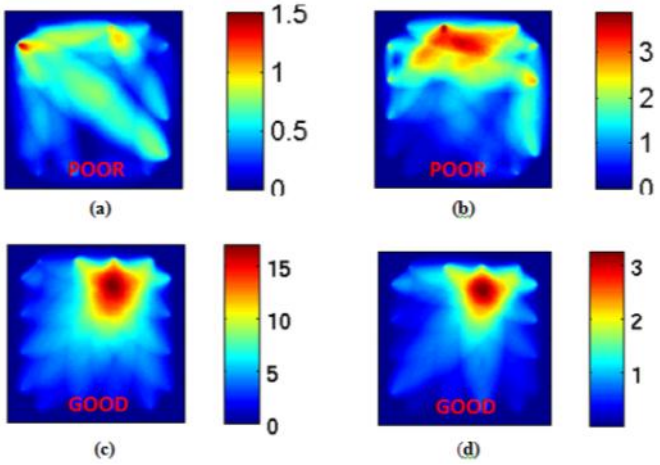

Figure 6: Sample tomogram images of defect state 8 in the aluminum plate, using various signal features: (a) Envelope peak time at 360 kHz, (b) FFT peak frequency at 210 kHz, (c) Signal energy at 80 kHz, (d) SDC at 260 kHz

The trend in the tomogram as the defect severity increases may reveal the sensitivity and robustness of a particular feature. If the feature is not robust, small changes in the size or geometry of the defect may dramatically affect the resulting image. Such nonlinear dependence on damage severity and geometry is undesirable. Two examples of such a trending comparison are shown in Figures 7 and 8 for a "good" and "poor" result, respectively. The series of eight tomograms in Figure 7 were generated for each of the eight defect growth states using the signal energy feature at 100 kHz, while those in Figure 8 were generated using the FFT peak frequency at 260 kHz. Noting the color scales in each image of Figure 7, it is clear that as the defect severity increases, and the maximum amplitude in the tomogram increases monotonically while the defect location on the tomogram remains constant. In Figure 8, the defect location is difficult to determine and the amplitude of the tomogram is inconsistent with the severity of the damage.

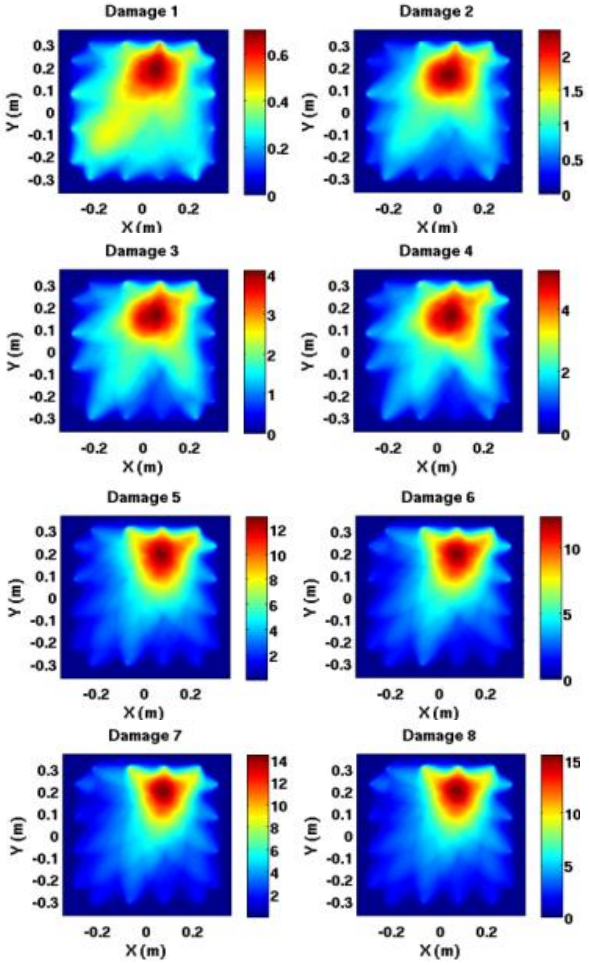

Figure 7: An excellent result, using the energy feature at 100 kHz, normalized to each defect image individually. Note the color scale limits.

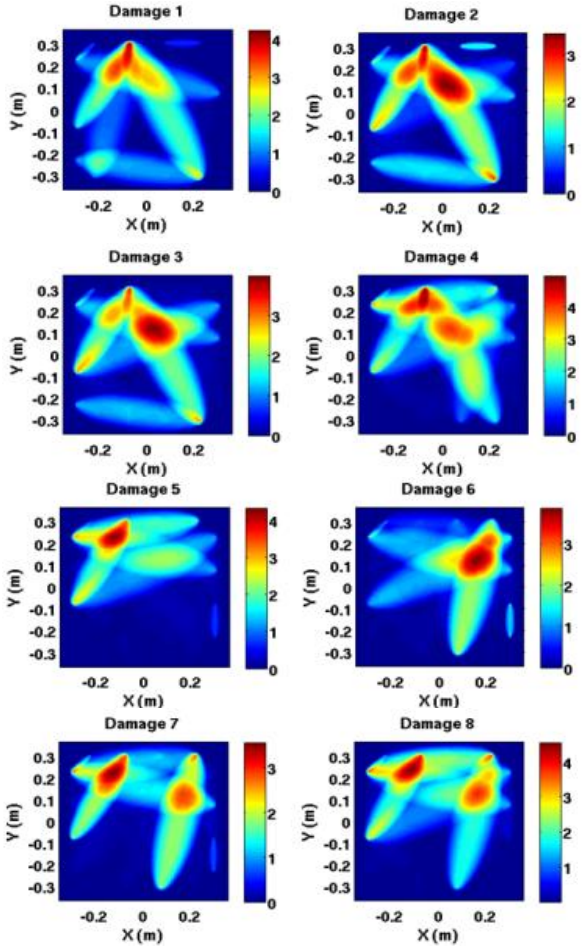

Figure 8: A poor result, using the FFT peak frequency feature at 260 kHz, normalized to each defect image individually. Note the color scale limits.

Signal Feature Comparison – Sensitivity to Temperature

In addition to the detection, localization, and trending capabilities of a signal feature, its sensitivity to damage versus its sensitivity to normal environmental fluctuations is also of key importance. In order to compare the sensitivity of various features to moderate temperature fluctuations as well as the eight defect growth states described above, baseline data (i.e. defect free) was collected over a period of several days with plate temperatures ranging from 66°F to 88°F. This is a relatively small temperature range but is sufficient to provide data for comparison between several features. The maximum tomogram image magnitude was compared for each of the selected signal analysis features as a function of damage state and temperature shift. Ideally, the tomogram magnitudes generated due to temperature shifts would be much smaller than those generated by small defects, thus allowing simple thresholding to account for most temperature effects. Examples of excellent and poor results are provided in Figures 9 and 10. In Figure 9 it is apparent that the temperature increases (ranging from 1°F to 22°F, labeled T1 through T5) resulted in minimal tomogram amplitudes compared to the amplitudes generated by the defect stages (labeled D1 through D8) using the FFT spectrum amplitude feature at 140 kHz. This is an excellent result with monotonic growth in the tomogram intensity with defect growth and very minimal influence by temperature. Therefore a threshold limit could be determined above which anomalies in the tomogram would be identifiable as damage-induced and not temperature-induced. In comparison, the same data was analyzed using the SDC feature at 360 kHz with poor results, as shown in Figure 10. Not only is the tomogram amplitude highly nonlinear with defect growth, but the tomogram amplitudes due to temperature variations exceed those induced by even the largest defects. This high sensitivity to temperature is due to the phase dependence of the SDC signal feature.

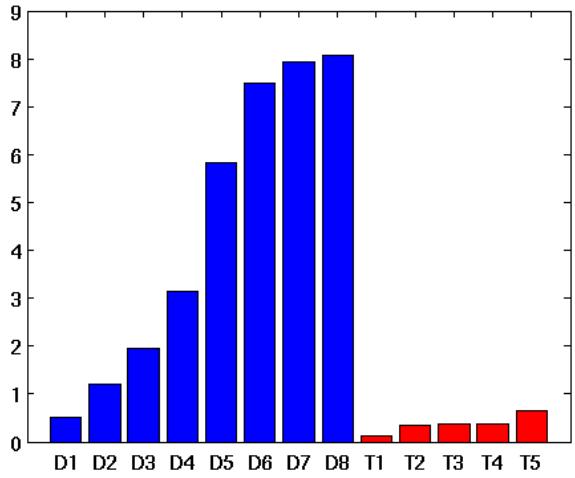

Figure 9: Comparison of the maximum tomogram amplitudes for various temperatures (red) and defect growth states (blue) using the frequency spectrum amplitude feature at 140 kHz.

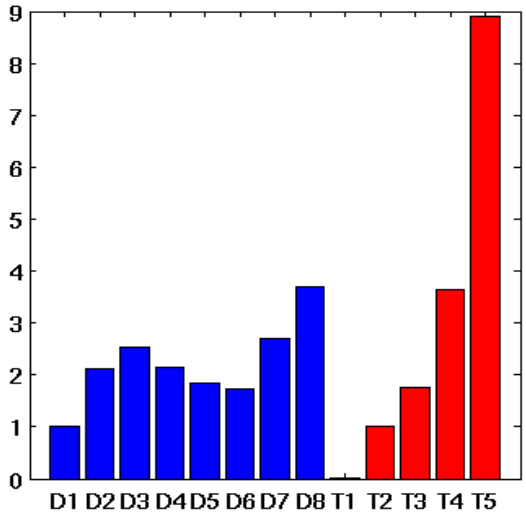

Figure 10: Comparison of the maximum tomogram amplitudes for various temperatures (red) and defect growth states (blue) using the SDC feature at 360 kHz.

EXPERIMENTAL RESULTS IN PSEUDO ARMOR PANELS

Tomographic Damage Detection Tests with Embedded Sensors

Sensors were embedded in a number of pseudo armor panels and ultrasonic data was collected under various states of damage. (Note that an image of the pseudo composite armor panel design is omitted intentionally.) A set of tomograms from a 12"-by-12" pseudo armor panel are shown for 5 increasing levels of damage in Figure 11. Here the damage is initially localized, but after repeated damage events at the same location, the damage spreads across the entire panel. This effect is accurately captured by the tomography algorithm, and, noting the changes in the color scale limits, the increasing severity of the damage is also captured. Here the FFT peak value feature was utilized at a central ultrasonic excitation frequency of 110 kHz. Note that images and photos and detailed descriptions of the pseudo composite armor panels and the damage mechanisms utilized during these tests are intentionally omitted.

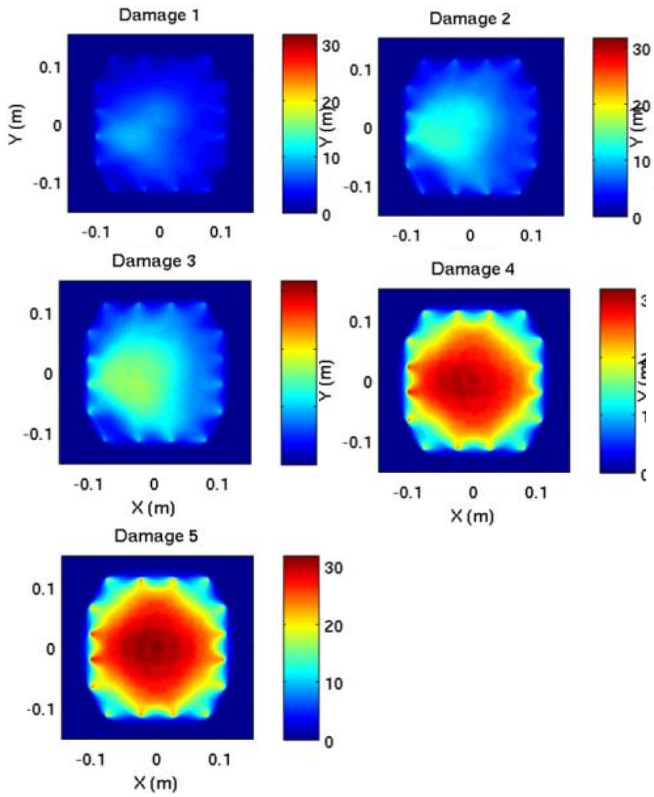

Figure 11: Tomograms from a pseudo armor panel with embedded sensors generated using the FFT spectrum peak value feature at 110 kHz for five increasing levels of damage.

Sparse Array Analysis

In addition to evaluating various signal features for tomographic analysis, efforts were made to reduce the number of required sensors by increasing the sparsity of the sensor array. The minimum number of sensors required per square foot of pseudo armor panel is dependent on a number of factors including penetration power of the sensors, required sensitivity to defects, the degree to which defect severity information is required, and the importance of precision in locating the defects. To analyze the effect of reducing the number of sensors in an array, a sparse array analysis was performed on the ultrasonic damage test data from a pseudo armor panel with embedded sensors. By selectively downsampling the number of sensors used during the tomography calculations, nine different sparse arrays having between 3 and 16 sensors, as shown in Figure 12, were evaluated for each damage state. The nine sparse array configurations were compared according to tomogram intensity, tomogram defect location accuracy, and ability to monotonically track damage severity, as shown in Figures 13 and 14.

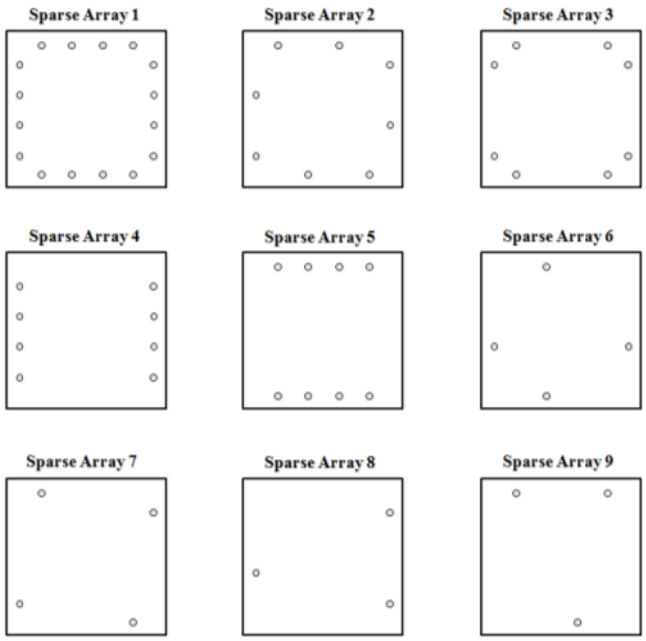

Figure 12: The nine different sparse array sensor configurations tested in the pseudo armor panel for five states of damage with increasing severity.

Tomograms of damage state 1 (the least severe damage state) are shown for each sparse array configuration in Figure 13. Here it is apparent that sparse arrays 1 through 5 produce tomograms that clearly show the presence and approximate location and extent of the damage, and that while the other arrays detect the damage, it is difficult to determine where that defect may be, what its severity might be, and whether or not it is a real indication of damage or simply an artifact due to a single anomalous signal. Figure 14 shows the trend in maximum tomogram intensity for each sparse array as the damage severity increases from damage state 1 to state 5. Note that for each of the sparse array configurations the amplitude increases quite consistently and that a large jump occurs after defect state 3. Therefore each of the sparse array configurations was capable of detecting and tracking the severity of the damage through each of the five damage states, although localization of the defect was more problematic with the sparser arrays. It is likely that due to the more global nature of the damage that occurred at damage state 3, the sparse arrays with fewer sensors were at less of a disadvantage in detecting the damage. In a case in which the defect is small and or highly localized, the very sparse arrays, such as those in configurations 6 through 9, may be more likely to miss the damage.

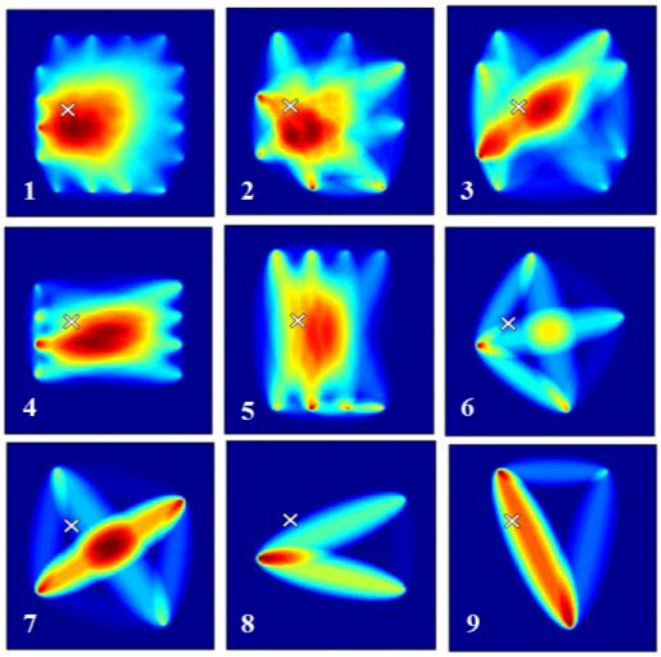

Figure 13: Tomograms from damage state 1 using the signal energy feature at 115 kHz for nine unique sparse sensor arrays, as detailed in Figure 12. The number in the lower left corner of each image indicates the sparse array configuration number and the white 'X' indicates the actual damage location.

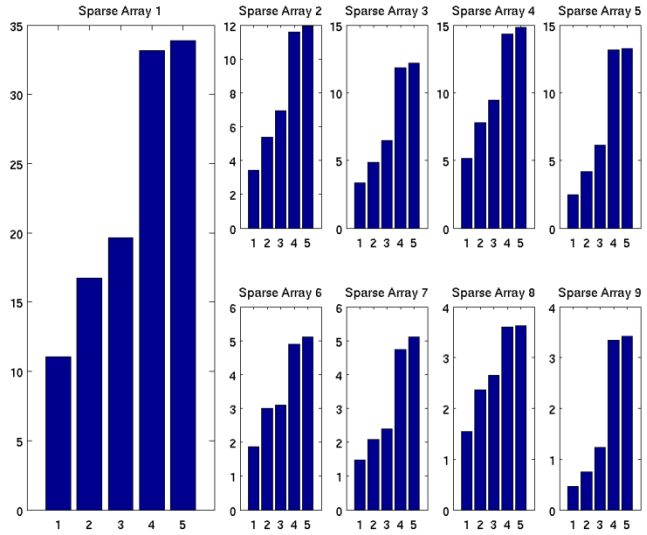

Figure 14: Trends of the maximum tomogram intensity for each of the nine sparse arrays as the damage severity was increased.

Based on the result of the sparse array tests in the pseudo armor panel (as well as similar tests in the representative aluminum plate), it was determined that with an

appropriately selected signal feature, very sparse arrays (with as few as 3 sensors per array) can still effectively detect small defects and track damage severity, although this is somewhat dependent on defect size and location. Based on this information and guided wave penetration power tests in several pseudo armor panels, FBS was able to recommend an approximate minimum sensor density of 3 to 4 sensors per square foot for a 12”-by-12” pseudo armor panel and a sensor density of 0.75 to 1 sensors per square foot for a 24”-by-24” pseudo armor panel. The differences lie in the fact that regardless of the panel size, at least 3 to 4 sensors are required to reliably detect damage and track damage severity. It is possible that 3 to 4 sensors could be utilized to monitor the health of a larger 36”-by-36” pseudo armor panel, but without further testing this cannot be reliably determined.

FINITE ELEMENT MODELING AND ANALYSIS SOFTWARE

In addition to experimental testing and development, FBS is developing a highly-automated finite element model generation and analysis program to be used in conjunction with Abaqus/Explicit commercial finite element software. This program is specifically dedicated to modeling guided wave propagation in pseudo composite armor panels between embedded ultrasonic sensors. This software will allow TARDEC personnel to further investigate a wide array of sensor configurations and sensor densities and to evaluate the sensitivity of various feature extraction and tomography algorithms to damage of varying form and severity. The general structure of this software is outlined in Figure 15. The general system design and testing methodology is outlined in Figure 16. This methodology incorporates a combination of empirical evaluation, finite element modeling, and experimental testing and evaluation to determine the appropriate design for an armor panel SHM system.

The users can input a variety of parameters for the simulation including armor panel geometry and material properties and embedded sensor design, configuration, and excitation options. Based on these inputs, the software generates a Python script, which is read executed by Abaqus to automatically generate a finite element model using the appropriate design and meshing algorithms selected by FBS. This model can then be submitted for processing by Abaqus/Explicit, and the results can be output to file, extracted by another Python script, and then post-processed using one or more signal processing algorithms to generate tomographic images from the simulations.

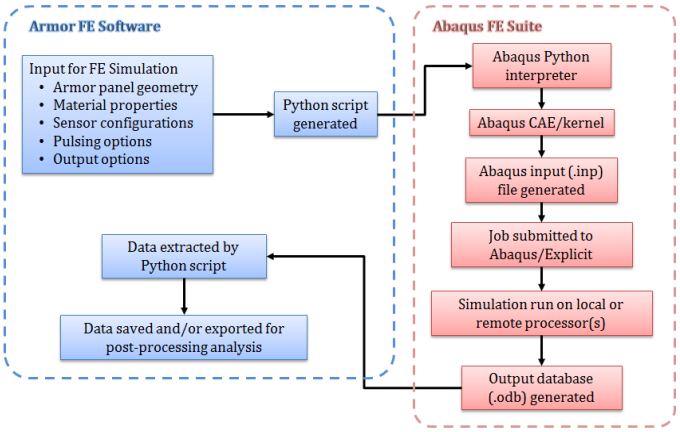

Figure 15: General outline of the finite element modeling and analysis package being developed by FBS, Inc. for generating, submitting, and analyzing finite element simulations of pseudo armor panels with embedded ultrasonic sensors in conjunction with the Abaqus/Explicit commercial finite element software.

FBS invested a substantial amount of effort into optimizing the model design, material properties, meshing algorithms, and excitation methods utilized in the software to assure accurate, reliable, and efficient model generation and execution for a variety of armor panel, sensor, and excitation parameters. One example of a meshed panel generated with FBS’s software in conjunction with Abaqus is shown in Figure 17 with six embedded sensors shown in blue.

One manner in which model verification was performed was guided wave velocity comparison. Ultrasonic guided wave signals measured in fabricated pseudo armor panels with embedded sensors were compared to those in similar simulated panels. The group velocity in the 0° direction in the panels was measured to be 4177 m/s ± 250 m/s and the group velocity calculated from the finite element data was 4030 m/s ± 127 m/s. Errors in velocity calculations arise from the determination of the precise point in time in which the wave packet arrives at a point in space as well as the inability to calculate a precise wave travel distance between sensors with a non-zero dimension in the wave propagation direction.

A sample result of a tomogram generated from a fabricated pseudo composite armor panel with an induced defect is provided in Figures 18 and 19; here six embedded sensors were utilized. This model representing this panel with similar embedded sensors and similar damage produced the tomogram (using similar signal processing) in Figures 20 and 21. Note that further model and experimental details and the specific damage mechanisms utilized in the tests are intentionally omitted.

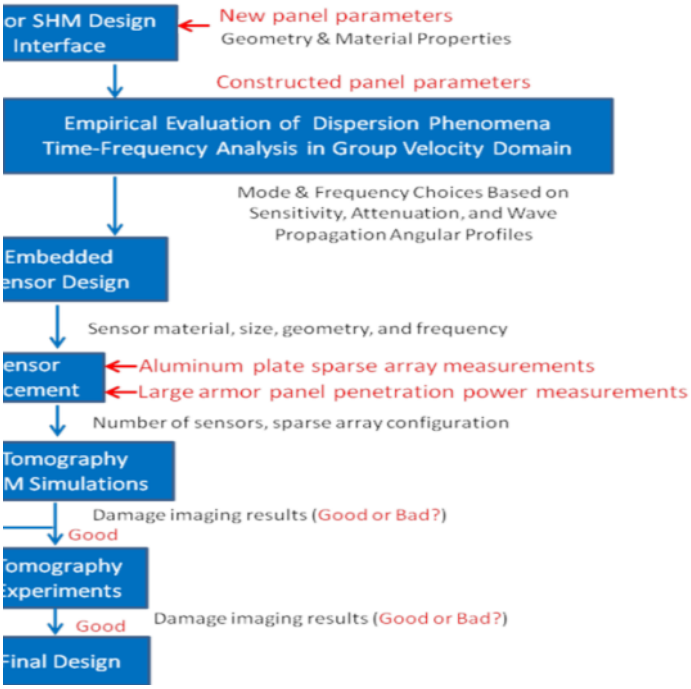

Figure 16: General methodology for armor panel SHM system design incorporating empirical evaluation, finite element modeling, and experimentation.

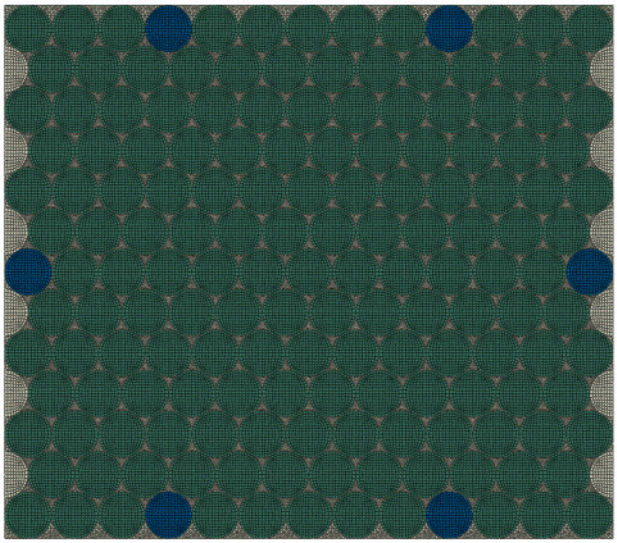

Figure 17: A meshed finite element model of a pseudo composite armor panel showing six embedded sensors in blue.

CONCLUDING REMARKS

FBS has demonstrated that embedding piezoelectric ultrasonic sensors in composite armor panels is technically feasible and that even sparse sensor arrays can provide excellent damage detection sensitivity and damage severity tracking using guided wave computed tomography as long as appropriate signal analysis features are utilized. Such sparse sensor arrays can provide high sensitivity to damage throughout the region of inspection and can be used to track the severity of damage. The implementation of such a system could provide real-time or periodic structural health monitoring of ground vehicle armor panels, likely with little to no compromise in armor weight or integrity. Future enhancements of this technology could include passive sensing to detect and locate impact events as well as acoustic emission structural health monitoring. Additionally, a highly-automated software package is being developed that will allow TARDEC personnel to generate, execute, and analyze finite element models of armor panels with embedded ultrasonic sensors. This software package will enable the users to investigate many armor geometries, sensor designs, excitation signals, and signal processing algorithms in composite armor panel models with defects of varying form and severity. Such extensive investigations would be impractical to carry out experimentally.

REFERENCES

[1] V. Giurgiutiu, *Structural Health Monitoring with Piezoelectric Wafer Active Sensors*, Academic Press, Burlington, MA, 2008.

[2] J.L. Rose, *Ultrasonic Stress Waves in Solid Media*, Cambridge University Press, Cambridge, UK, 2004.

[3] UltraWave LRT, Olympus NDT (accessed July 8, 2013), http://www.olympus-ims.com/en/ultrawave/.

[4] H. Gao, F. Yan, J.L. Rose, X. Zhao, C. Kwan, and V. Agarwala, "Ultrasonic Guided Wave Tomography in Structural Health Monitoring of an Aging Aircraft Wing", *ASNT Fall Conference and Quality Testing Show Proc. 2005*, pp. 412-415.

[5] T.R. Hay, R.L. Royer, H. Gao, X. Zhao, and J.L. Rose, "A comparison of embedded sensor Lamb wave ultrasonic tomography approaches for material loss detection", *Smart Structures and Materials*, Vol. 15, p. 946-951, 2006.

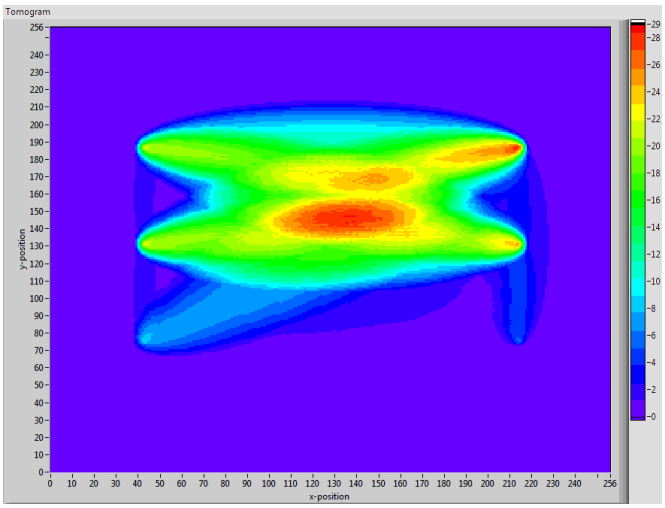

Figure 18: A tomogram generated from experimental data from a pseudo armor panel with six embedded sensors showing the location of an instance of induced damage.

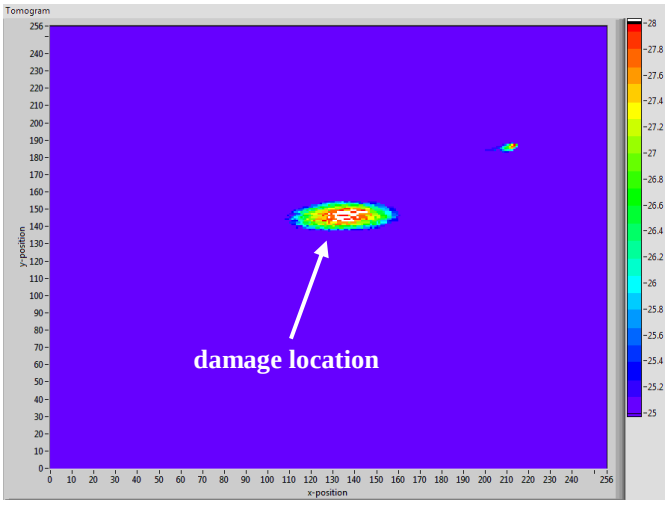

Figure 19: The same tomogram from Figure 18 with amplitude thresholding applied.

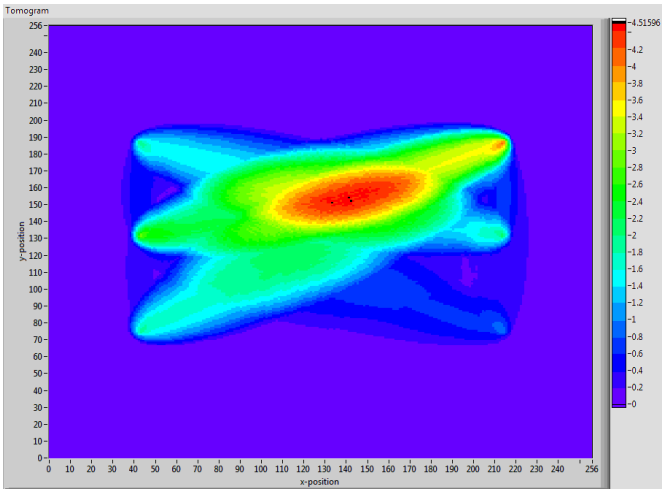

Figure 20: A tomogram generated from numerical finite element modeling data from a pseudo armor panel identical to the panel imaged in Figure 18 showing the location of an instance of simulated damage.

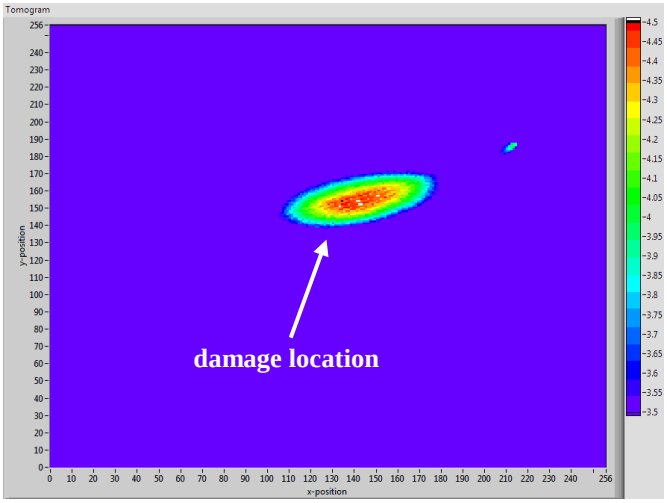

Figure 21: The same tomogram from Figure 20 with amplitude thresholding applied.

DISCLAIMER: Reference herein to any specific commercial company, product, process, or service by trade name, trademark, manufacturer, or otherwise, does not necessarily constitute or imply its endorsement, recommendation, or favoring by the United States Government or the Department of the Army (DOA). The opinions of the authors expressed herein do not necessarily state or reflect those of the United States Government or the DOA, and shall not be used for advertising or product endorsement purposes.